

22288

Estimation of eddy diffusivity coefficient of heat in the upper layers of equatorial Arabian Sea

P O Zavialov*

State Oceanographic Institute, Kropotkinsky Pereulok, 6 Moscow, Russia

and

V S N Murty

National Institute of Oceanography, Dona Paula, Goa 403 004, India

Received 26 September 1994; revised 23 June 1995

A 1-D model for estimating eddy diffusivity coefficient of heat (K_h) in the upper layers of the sea is proposed and tested using data collected along 68°E and 52°E in the equatorial Arabian Sea. Diurnal range of sea surface temperature in this region is up to 0.4°C with minimum temperature occurring at 0630 hrs IST and maximum temperature occurring at 1600 hrs IST. The value of K_h is found to vary between 0.003 and 0.011 $m^2 s^{-1}$ with lower value in the Central Equatorial Arabian Sea (CEAS). A comparison of the model computed K_h values with those estimated from the heat balance of the upper layer (50 m) of the sea shows good agreement in the region of weak winds (CEAS) or low turbulent mixing regime. Computed K_h is found to be slightly lower than the estimated K_h in the region of strong winds (Western Equatorial Arabian Sea) or high turbulent mixing regime.

Studies on the diurnal cycle for an accurate coupling between the ocean and atmosphere are gaining importance¹⁻³. The contribution of energetic diurnal cycle to the mean daily heat flux through the mixed layer is shown to be considerable¹. Observations of sea surface temperature (SST) show a diurnal range up to a maximum of about 2°C in the western equatorial Pacific² and a smaller value of about 0.2°C in the central equatorial Pacific³. The diurnal range of SST is about 0.5°C during south-west monsoon in the Arabian Sea (off Karwar)⁴ and about 1.3°C during pre-onset of monsoon in the eastern Arabian Sea⁵. Within the surface mixed layer the diurnal amplitude of temperature decreases with depth and the rate of decrease depends mainly on the eddy diffusivity coefficient of heat (K_h ; this term is widely used compared to eddy conductivity of heat or coefficient of turbulent exchange of heat). Bowden *et al.*⁶ and Pivovarov & Protasov⁷ have estimated K_h for the Atlantic Ocean and Black Sea respectively from the surface meteorological observations and the diurnal variation of temperature in the upper layers. Similar studies are few for the Indian seas.

Zavialov & Rozhdestvensky⁸ developed a coupled 1-D model (hereafter referred to as ZR⁸

model for simulating the diurnal cycle of temperature in the boundary layers of tropical ocean and atmosphere in which the coefficient K_h is supposed to be known and is used as an input parameter for the estimation of temperature variation, $T(z, t)$, as a function of both depth (z) and time (t). In the present paper, an attempt has been made to parametrize K_h by inverting the ZR model and a new method (1-D model) for estimating the daily and depth averaged K_h in the upper layers of the ocean is proposed. This method is based on observations of diurnal variation of temperature, $T(z, t)$ at different levels in the upper layers ($z=50$ m thick) of the equatorial Arabian Sea which are used as an input parameter to estimate the value of K_h (Method 1). The model computed K_h is then compared with that estimated from the heat balance of the upper layers (Method 2) of the equatorial Arabian Sea.

Materials and Methods

Method 1 (1-D model)

The ZR model simulates the diurnal cycle of temperature in the boundary layers of the atmosphere and sea by considering the known values of turbulent diffusivity coefficients in the air (K_1) and water (K_h). The coefficient K_1 is assumed to in-

*Present address: Department of Physics, University of Rio Grande, CXPostal 474, Rio Grande RS, CEP 96201-900, Brazil

crease linearly with height over the surface, while K_h is assumed to be constant with respect to depth and time. It is assumed that the temperature variations in these media are produced by vertical diffusivity of heat (1-D model), the incoming solar radiation (containing both the visible and infrared wavelengths), an outgoing latent, sensible and longwave heat flux at the surface. Horizontal advection of heat is neglected. The model accounts for absorption of solar energy as a spectral function of depth within the upper layer. While the infrared radiation is absorbed in the top few centimetres below the sea surface, the visible part of the spectrum penetrates to deeper depths with decreasing intensity⁹. For the computation of the energy that reaches a given depth it is necessary to know the intensity of the radiation at different wavelengths, i.e. energy spectrum. The reduction in the energy for each wavelength range with depth is considered to be approximately exponential and is to be calculated using individual attenuation coefficient. The total energy reaching the given depth is then calculated by summation⁹.

In accordance with the physics described above, the governing equations of the ZR model are as follows.

$$\frac{\partial T_1}{\partial t} = \frac{\partial K_1}{\partial z} (1 - \mu z) \frac{\partial T_1}{\partial z}; \quad z < 0 \quad \dots (1)$$

and

$$\frac{\partial T_2}{\partial t} = K_h \frac{\partial T_2}{\partial z^2} + \frac{1-A}{C_2 \rho_2} J(t) \sum_{m=1}^M j_m \beta_m e^{-\beta_m z} \quad \dots (2)$$

where

$T_1(z, t)$ and $T_2(z, t)$ = temperature of air and sea water respectively, z = vertical coordinate (Z axis is directed downwards and its origin lays at surface), t = time, μ = coefficient (0.3 m^{-1}) describing the rate of increase of K_1 with the height over the ocean, ρ_2 = density of seawater (1000 kg m^{-3}), C_2 = specific heat of seawater ($4000 \text{ J kg}^{-1} \text{ K}^{-1}$), A = albedo of ocean surface.

The second term in the RHS of Eq. (2) corresponds to the volume absorption of solar radiation $J(t)$ in water as described above. The solar spectrum is divided into narrow spectral ranges and radiation within each range is considered to be monochromatic¹⁰. For the m^{th} wavelength range, its specific weight in the spectrum (in fractions of unity) j_m and the corresponding absorption coefficient β_m are considered.

The above Equations (1) and (2) are supplemented with the following boundary conditions:

(i) The requirement of equality of temperature T_1 and T_2 at the interface, i.e. $T_1(0, t) = T_2(0, t)$

(ii) Determination of constant temperature of water at asymptotically deep level at which diurnal changes of temperature are no longer measurable, i.e. $T_2(\infty, t) = f$

(iii) Heat balance of the sea surface, i.e.

$$C_2 \rho_2 K_h \frac{\partial T_2}{\partial z}(0, t) - C_1 \rho_1 K_1 \frac{\partial T_1}{\partial z}(0, t) = F(0, t) + L \rho_1 K_1 \frac{\partial q}{\partial z}(0, t) \quad \dots (3)$$

where C_1 and ρ_1 are the specific heat ($1005 \text{ J kg}^{-1} \text{ K}^{-1}$) and density (1.3 kg m^{-3}) of air, respectively, and $F(0, t)$ is the effective infrared radiance at surface, which may be parametrized through the sea surface temperature as

$$F = \delta \sigma T_2^4(0)$$

where δ is the coefficient (0.97) which accounts for 'non-blackness' of the sea surface and σ the Boltzmann's constant ($567 \times 10^{-10} \text{ W m}^{-2} \text{ K}^{-4}$). The last term of Eq. (3) describes the latent heat flux, where L is the specific heat of vaporization ($2441 \times 10^3 \text{ J kg}^{-1}$) and $q(z, t)$ the vertical profile of air humidity.

(iv) The condition of asymptotic decrease of vertical heat flux with the distance from surface, i.e.

$$\frac{\partial T_1}{\partial z}(\infty) = \frac{\partial T_2}{\partial z}(\infty) = 0 \quad \dots (4)$$

Equations (1 and 2) have an analytical solution expressed as a sum of Fourier modes. The mathematical details are described elsewhere^{8,10}. The parametrization of the diurnal cycle of temperature $T_2(z, t)$ in the upper layers of the sea is represented as the sum of the daily averaged temperature as a function of depth and the real part of Fourier series of the amplitude of daily variation of temperature at depth, z and is given as:

$$T_2(z, t) = \bar{T}_2(z) + \text{Re} \sum_{m=1}^M V_n(z) e^{-in\omega t} \quad \dots (5)$$

where, \bar{T}_2 = daily averaged temperature as a function of depth; $V_n(z)$ = complex amplitude of n^{th} Fourier term of the daily temperature variation at

depth, z and its mathematical details are given elsewhere^{8,10}; $n=n^{\text{th}}$ Fourier term; and ω =frequency corresponding to the diurnal period.

The Eq. (5) provides the model parametrization for the diurnal cycle of water temperature considering the known eddy diffusivity K_h .

In the present study the model described above is inverted and proposed the method to find the unknown K_h from the diurnal cycle observed *in situ* by considering the same (i-iv) boundary conditions. It is clear from the physics that the rate of decay should depend primarily on the intensity of vertical mixing, i.e. on K_h . Indeed, if mixing is weak, the daytime surplus of solar heat is 'trapped' in top few metres, leading to diurnal amplitudes large at surface, but abruptly decreasing with the depth. In contrary, if mixing is strong, the surplus heat is distributed nearly uniformly over the mixed layer, resulting in relatively weak, but nearly uniform diurnal amplitudes, i.e. the decay of the diurnal cycle with depth is slow. Thus the vertical distribution of diurnal temperature variations is a natural indicator of intensity of mixing.

The following expressions can be obtained directly from the solutions of equations given for $V_n(z)$ above^{8,10}.

$$\left| \frac{V_n(0)}{V_n(z_0)} \right| = \frac{\sum_{m=1}^M \frac{j_m \beta_m}{K_h \beta_m^2 + in\omega} \left(1 + \frac{\beta_m \sqrt{2K_h}}{\sqrt{n\omega} (i-1)} \right)}{P(z_0)} \quad \dots (6)$$

where

$$P(z_0) = \left| \sum_{m=1}^M \left[\sqrt{\frac{2K_h}{n\omega}} \cdot \frac{\beta_m}{i-1} \cdot \exp \left(\sqrt{\frac{n\omega}{2K_h}} (i-1) z_0 \right) + \exp(-\beta_m z_0) \right] \frac{j_m \beta_m}{K_h \beta_m^2 + in\omega} \right| \quad \dots (7)$$

and $V_n(0)$ and $V_n(z_0)$ are the complex amplitudes of n^{th} Fourier term of daily temperature variation at surface and at the depth z_0 respectively. Thus, if $V_n(0)$ and $V_n(z_0)$ are known from temperature observations, the transcendent Eqs (6 and 7) can be solved to find out K_h .

It would be the best to take β and j values from direct measurements in the equatorial Arabian Sea. However, no information is available on the spectral characteristics and absorbing conditions of the solar irradiance in the seawater for the study region. Because of this, in the present study the values of β and j estimated for the Black

Sea^{8,11} during summer time have been considered. Also it would be better to take M (wavelength range) as large as possible; but due to limitation of such data only three wavelength ranges have been considered following Voskanyan *et al.*¹¹. Therefore the values considered are: $M=3$; $j_1=0.24$, $j_2=0.23$, $j_3=0.53$; $\beta_1=0.1 \text{ m}^{-1}$, $\beta_2=0.9 \text{ m}^{-1}$ and $\beta_3=4.9 \text{ m}^{-1}$. This is acceptable because, in the structure of the equations, the K_h value depends more strongly on $V_n(0)$ and $V_n(z_0)$ than on β and j values. This indicates that even if we consider the exact values of β and j of the equatorial Arabian Sea (if available), the final solution for K_h will not be affected much.

Method 2 (for comparison with Method 1)

This method is based on the equation of heat balance of the upper layers of the sea (with incoming solar radiation as heat gain at sea surface, the fluxes of latent heat, sensible heat and effective long wave radiation as heat losses at sea surface, and vertical heat flux across the base of the upper layer as heat gain/loss to/from the above layer) in which the horizontal advection of heat flux is supposed to be insignificant. The heat gain (ΔH) in the water column over the period of $\Gamma=24$ hours ($=86400$ s) may be written as

$$\Delta H = (Q_N - Q_{\text{Bott}}) \Gamma \quad \dots (8)$$

and following Stevenson¹² and Voskanyan *et al.*¹¹, the Q_N and Q_{Bott} can be expressed, respectively, as

$$Q_N = Q_0 - Q_B - Q_H - Q_E \quad \dots (9)$$

$$Q_{\text{Bott}} = -K_h(z_0) C_2 \rho_2 \frac{\partial \bar{T}_2}{\partial z}(z_0) \quad \dots (10)$$

where

Q_N =net heat flux at the sea surface; Q_{Bott} =turbulent heat flux across the base of the chosen layer; Q_0 =solar radiation at sea surface corrected to cloud cover and the albedo at sea surface; Q_B =net long wave radiation at the air-sea interface; Q_H =sensible heat flux at the air-sea interface; Q_E =latent heat flux at the air-sea interface; \bar{T}_2 =daily averaged value of temperature as function of depth, z ; z_0 =the depth of the base of the chosen layer.

The heat gain (ΔH) of the water column can be estimated from the heat content of the upper layer as

$$\Delta H = H_{24} - H_{00} \quad \dots (11)$$

where H_{00} and H_{24} are the heat contents of the layer (surface to z_0) at 0000 hrs and at 2400 hrs respectively and can be expressed¹³ as

$$H = \rho_2 C_2 \int_{\text{surface}}^{z_0} T_2 dz \quad \dots (12)$$

Substitution of Eq. (10) into Eq. (8) gives directly the following formula for estimating $K_h(z_0)$ as

$$K_h(z_0) = \frac{1}{\Gamma C_2 \rho_2 \frac{\partial \bar{T}_2}{\partial z}(z_0)} (Q_N \Gamma - \Delta H) \quad \dots (13)$$

Following this procedure the depth averaged values of K_h for different levels of z_0 are obtained (caution: it is supposed here that the total amount of solar irradiance is being absorbed in the surface homogeneous layer, so z_0 must be below this layer).

This method should be used for the time-series temperature data at a fixed location. However, in the present study, as outlined later, this method is used by assuming that the observed changes in the heat content are only due to the action of heat fluxes over the diurnal period rather than spatial variability along the ship's track. In other words, the temperature changes are supposed to be dominated by temporal trend and diurnal cycle rather than by spatial variability along the ship's track.

Data

The validation of the present model to compute K_h requires time series of temperature data at a stationary position. However, for computing K_h from this model, the upper layer temperature data collected at 16 closely spaced (≈ 50 km) stations along 68°E and 52°E sections (Fig 1) in the equatorial Arabian Sea on 22, 23 and 30 August, 1991 on board *ORV Sagar Kanya* under Indo-USSR collaboration programme have been utilized, as there were no time series data during the survey period (18 Aug.-20 Sept. 1991). The time taken by the vessel to cover the distance between the stations was about 4 h and at each station the sampling was done within 40 min. At each station the temperature data were obtained using a CTD (Sea-Bird, USA, Accuracy: $\pm 0.002^\circ\text{C}$) system. Precautions were taken to lower the CTD at a slower rate in the top 200 m depth as the temperature changes are rapid in the water column.

The surface meteorological data at the stations were used to compute the heat balance components. The air temperature (dry and wet bulb) was

measured at 10 m height above the sea surface using an un aspirated psychrometer. The wind (direction and speed) was measured at a height of 22.6 m above the sea surface and hence, a height correction¹² was applied to reduce it to the standard height of 10 m above the sea surface.

The daily averaged solar radiation reaching the sea surface (Q_s) was computed utilizing an empirical formula¹⁴ and was corrected to cloud cover¹² and albedo¹⁵ at sea surface to get Q_0 , the daily average value of solar irradiance penetrating below the sea surface. The parameter Q_0 is given by $Q_0 = Q_s(1 - A)$ where 'A' is the albedo at the sea surface. The heat balance components such as net long wave radiation (Q_B) sensible heat flux (Q_H) and latent heat flux (Q_E) were computed with the individual set of observations utilizing the bulk aerodynamic formulae given by Stevenson¹² with the exchange coefficients for moisture (C_E) and heat (C_H) corrected for wind speed¹⁶ and atmospheric stability¹² and were averaged daily.

The net heat flux (Q_N) at the sea surface was estimated from Eq. (9). The heat content in the upper 50 m was computed from Eq. (12) using the temperature data with 5 m intervals.

Procedure for separation of diurnal cycle

The observed temperature changes along the ship's track contain both spatial, temporal, diurnal variations and temporal trend of longer period. For computing K_h from the model (Method 1), the diurnal cycle at each depth level is separated out from the observed temperature data (along 68°E and 52°E sections) by assuming the aperiodic part of variation of temperature along the ship's track (along 68°E and 52°E sections) and the trend of larger temporal scale to be approximately linear. There are 6 observations on 22 August and 5 observations each on 23 and 30 August spanning the diurnal period (00-24 hours) of the day (see ob-

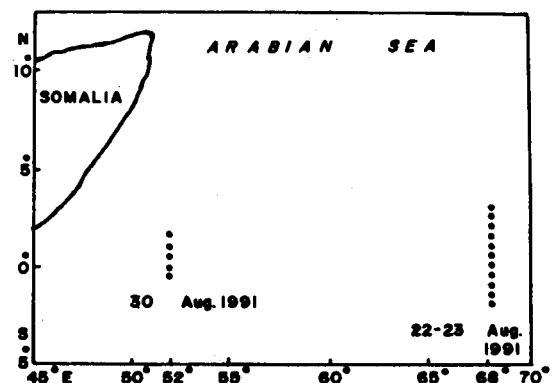


Fig. 1—Station locations

servation timings in Fig. 2). First, the deviations of observed temperature (at the stations) from the daily mean temperature at different depths are estimated. If the starting and ending observations of the day are taken at other than 0000 hrs and 2400 hrs, respectively, the deviations of temperature at these hours can be estimated from the temperature deviation curve by linear extrapolation from the time of first station to 0000 hrs and from the time of last station to 2400 hrs. The range of temperature deviation from 0000 hrs to 2400 hrs represents the amplitude of the aperiodic trend. Secondly, by assuming the aperiodic part of variation to be approximately linear, a line passing through the deviation values at 0000 hrs and 2400 hrs is constructed which gives rise to the linear trend of temperature over the diurnal period. From this line and the amplitude of aperiodic trend, one can estimate by linear interpolation the aperiodic part of variation of temperature at the time of observations over the diurnal period. Thus obtained aperiodic trend of temperature deviation value is then subtracted from the observed temperature deviation value over the diurnal period to get the diurnal cycle of temperature curve.

Results and Discussion

The thermal structure in the upper 50 m along 68°E and 52°E sections is presented in Fig. 2. The isotherms are drawn at interval of 0.2°C. Along 68°E (Fig. 2a) temperature decreased southward in the upper 20 m. Higher temperature regimes occurred during afternoon (1330-1600 hrs) and late night (0100-0300 hrs) while lower temperature regimes during morning (0530-0630 hrs) and night (2030-2230 hrs). Below 20 m depth, warm (>29.0°C) waters are seen between 2°N and Equator. Much lower temperatures (<27.5°C) are encountered at 50 m in the south.

Along 52°E the isotherms are nearly vertical (Fig. 2b). Very low temperatures (24.4-25.0°C) are noticed at 1°N. Temperature increased towards north and south of 1°N with relatively higher temperatures in the south.

Figure 3 represents a composite (2-day averaged; 22 and 23 August along 68°E) of the deviation of observed temperature (non-separated) over the diurnal period at different depths in the upper 50 m. The shape of the temperature deviation curve at 1 m depth (Fig. 3a) is noteworthy and indicates variation with a maximum positive deviation at 1400 hrs IST and a maximum negative deviation at 2400 hrs IST. This variation is not closed in the sense that the minimum deviation at

2400 hrs IST is not followed by the same deviation at 0000 hrs IST and in fact at 0000 hrs IST the deviation is positive. This is due to the component of aperiodic variation which can be noticed to decrease linearly (shown by broken line in Fig. 3a) from 0000 to 2400 hrs IST. The range of temperature deviation is less (0.15°C) between 0000 and 1200 hrs IST and is higher (0.34°C) between 1400 and 2400 hrs IST. The temperature curve at 5 m (Fig. 3b) is similar to that at surface up to 1400 hrs IST. The range of temperature deviation between 1400 and 1900 hrs IST is about 0.28°C and 0.2°C at 5 m and 10 m (Fig. 3c) respectively. At and below 15 m (Fig. 3d-f) the range of temperature deviation varies between 0.34°C and 0.37°C.

Figure 4 represents a composite (derived from Fig. 3) of the deviation of temperature of the (separated) diurnal cycle at different depths. The diurnal cycle close to the sea surface (Fig. 4a) is well depicted with a range of about 0.4°C. The minimum temperature deviation occurs at 0630 hrs IST and the maximum of deviation at 1600 hrs IST. Similar observations are reported in the eastern Arabian Sea⁵ and in the western equatorial Pacific². As expected one can notice the decrease in the amplitude of diurnal cycle of temperature with depth. However, no phase shift in the occurrence of maximum temperature deviation is noticed.

Figure 5 represents the diurnal variation of net long wave radiation (Q_B), sensible heat flux (Q_H) and latent heat flux (Q_E) along 68°E on 22 August and along 52°E on 30 August. Along 68°E, in the central equatorial Arabian Sea (CEAS), Q_H and Q_E increased gradually with time except a dip at 1330 hrs IST whereas Q_B decreased from 0200 to

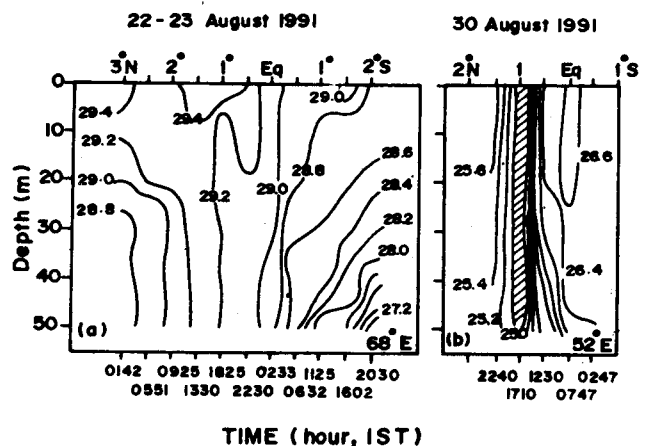


Fig. 2—Thermal structure in the upper 50 m along a) 68°E and b) 52°E

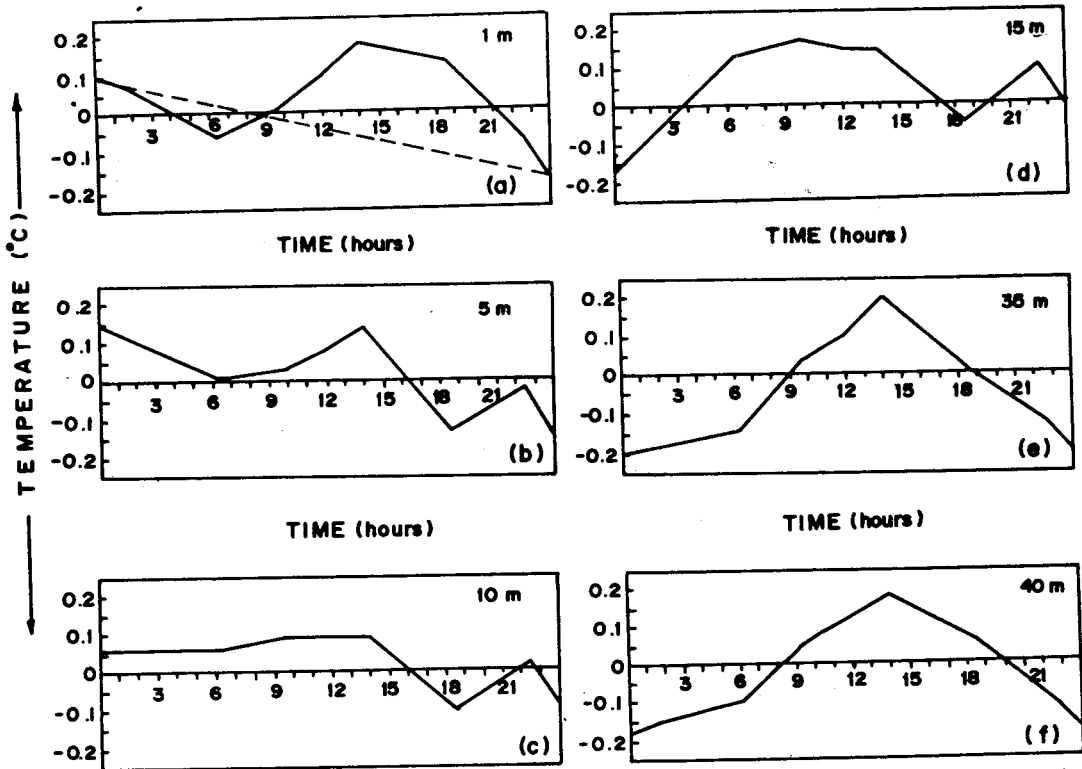


Fig. 3—A two-day (22 and 23 August) composite of deviation (actual-mean) of observed temperature (non-separated) over the diurnal period of different depths (The dashed line represents the aperiodic trend of variation over the diurnal depths)

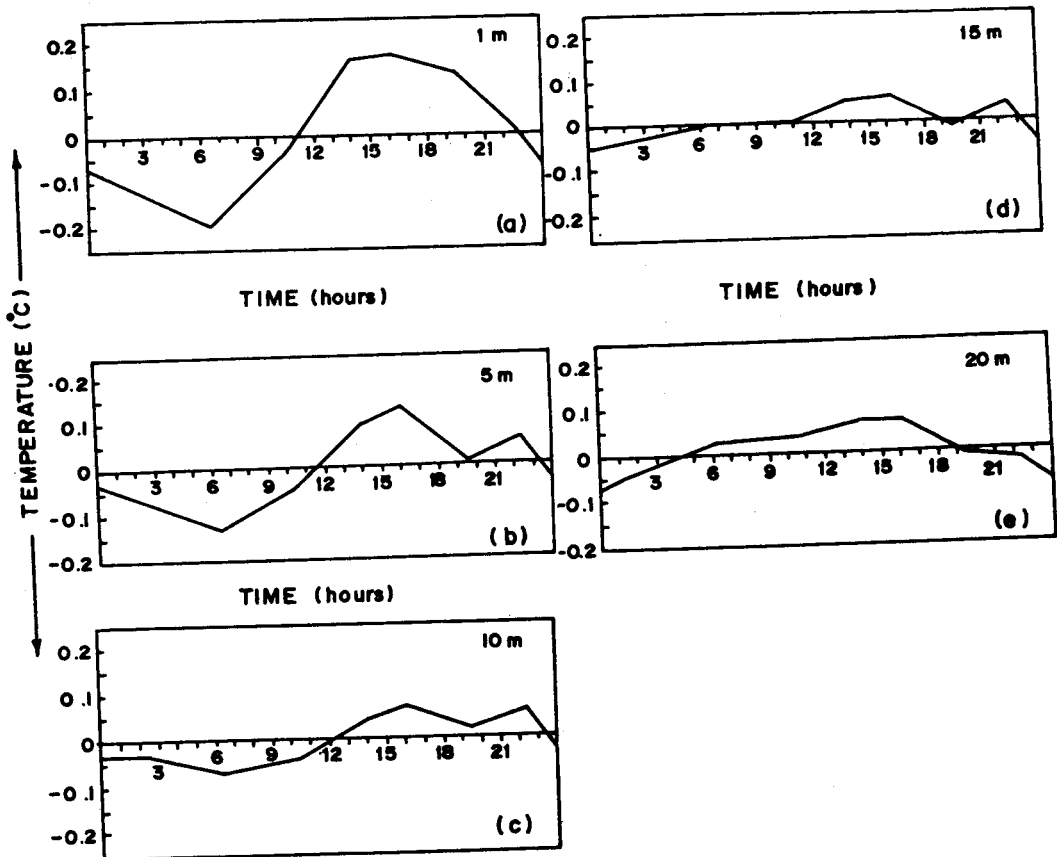


Fig. 4—A two-day (22 and 23 August) composite of deviation of temperature of the (separated) diurnal cycle of different depths

1330 hrs IST and increased slowly thereafter. The range of Q_E variation is less than 25 W m^{-2} . Along 52°E , in the western equatorial Arabian Sea (WEAS), Q_B , Q_H and Q_E decreased from 0300 to around 1700 hrs IST and increased slightly by 2300 hrs IST. The range of Q_E variation is considerably high (165 W m^{-2}). While the large Q_E (190 W m^{-2}) resulted from higher wind speeds (10 m s^{-1}), the low Q_E (25 W m^{-2}) is due to the low specific humidity gradients (between sea surface and 10 m height above it) over the lower SST ($< 25.0^\circ\text{C}$) region.

Table 1 shows the daily averages of solar radiation (Q_0), the total heat loss (Q_t) due to Q_B , Q_H , Q_E and the net surface heat flux (Q_N) along 68°E and 52°E . The slightly lower (266 W m^{-2}) solar radiation along 68°E and 52°E . The slightly lower (266 W m^{-2}) solar radiation along 68°E compared to 290 W m^{-2} along 52°E is due to higher mean cloud amount (about 4 octas) along 68°E than that along 52°E . The excess solar radiation over the total heat loss leads to positive net surface heat flux, indicating that the sea surface gains heat (heat flux into the sea). The heat flux into the sea is about 130 W m^{-2} and 150 W m^{-2} along 68°E and 52°E , respectively, and is nearly half of the solar radiation received at the sea surface. Rao *et al.*⁵ also reported similar observation during July-August of Monsoon-77 in the eastern Arabian Sea.

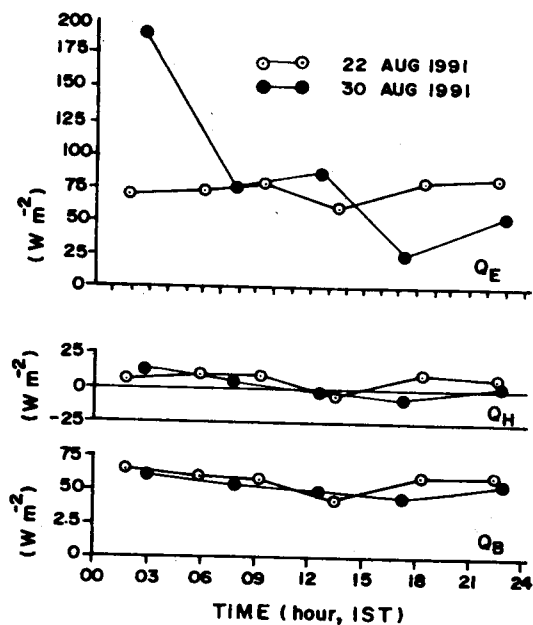


Fig. 5—Diurnal variation of net long wave radiation (Q_B), sensible heat flux (Q_H) and latent heat flux (Q_E) on 22 August, 1991 along 68°E and on 30 August, 1991 along 52°E

Figure 6 indicates the composite of heat flux (Q_{Bot}) profile in the upper 50 m computed from Eq. (10) after computing $K_h(z_0)$ from Method 1. The heat flux in the top 10 m is influenced by the wake of the ship's movement and the ship's draught¹⁷. The heat flux is high ($> 120 \text{ W m}^{-2}$) in the depth interval 10-20 m. The surface heat balance components also led to similar magnitude of heat flux into the sea. The shape of the heat flux profile also contains information on the profile of

Table 1—Daily estimates of heat budget components (W m^{-2}) at 68°E , 52°E in the equatorial Arabian Sea on 22, 23 and 30 August 1991

Date	No. of stations	Q_0	Q_t	Q_N
Along 68°E				
22 Aug. 91	6	267	136	131
23 Aug. 91	5	265	129	136
Along 52°E				
30 Aug. 91	5	289	141	148

Q_0 = solar radiation at the sea surface;
 $Q_t (= Q_B + Q_E + Q_H)$ = total heat loss across the air-sea interface;
 Q_N (+ve into the sea) = net surface heat flux

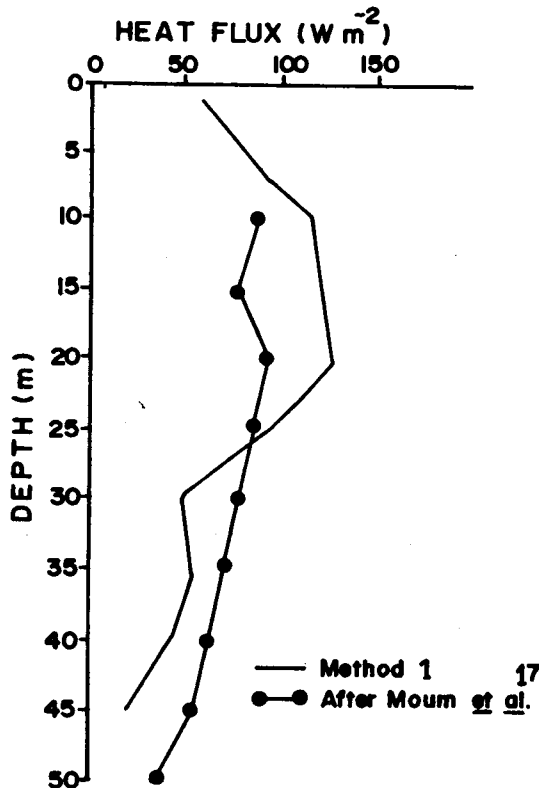


Fig. 6—A composite of computed heat flux profile from Method 1 in the upper 50 m [The heat flux profile after Mounm *et al.*¹⁷ is also shown]

K_h . The K_h value in the depth interval 10-20 m would be higher since low vertical temperature gradients are present in this layer (Fig. 2). Similarly, the K_h value below 20 m would be small as the heat flux is low and the vertical temperature gradients are higher (Fig. 2). A comparison between the computed heat flux profile (from the model) and the typical heat flux profile of the equatorial Pacific Ocean¹⁷ reveals a qualitative agreement between the two profiles. This emphasizes that the estimates from the present model are within the limits of observational results.

Figure 7 presents a comparison between the depth averaged K_h computed from the model (Method 1) and the estimated K_h from the heat budget (Method 2) for the upper 50 m water column corresponding to 22 and 23 August along 68°E and 30 August along 52°E. The diagonal passing through the origin represents one-to-one correspondence between the computed and estimated K_h values. The extreme left point (triangle) represents the K_h value for the Black Sea. Utilizing also the observations on diurnal variations of temperature in the Black Sea^{7,11}, the value of K_h was computed through Method 1. Earlier, using the same data the value of K_h was estimated^{7,11} through the method which was very close to our Method 2. A comparison of these values for Black Sea shows good agreement between the model computed and the estimated K_h values. This suggests the validity of the present model. Figure 7 also reveals close agreement between the computed K_h and the estimated K_h on 22 and 23 August along 68°E in CEAS.

Compared to the values of K_h in CEAS both the Methods 1 and 2 show relatively higher values of K_h on 30 August in WEAS where surface winds, solar radiation and net surface heat flux are high. This notifies that with the increase of wind speed from 2-3 m s⁻¹ in CEAS to above 10 m s⁻¹ in WEAS the K_h value is also increased in WEAS. This must be due to the increased turbulent efficiency of stirring associated with winds combined with wave-induced orbital motion, the magnitude of which also increases with wind speed¹⁸. However, in WEAS the model computed K_h (0.0105 m² s⁻¹) is lower than that estimated K_h (0.0155 m² s⁻¹) and shows that the model computed daily and depth averaged K_h is slightly underestimated (by about 33%). In other words, the estimated K_h is overestimated (by about 48%). This weaker agreement between the computed and estimated values of K_h in WEAS and the better agreement between them in CEAS probably results from the higher turbulent mixing regime due

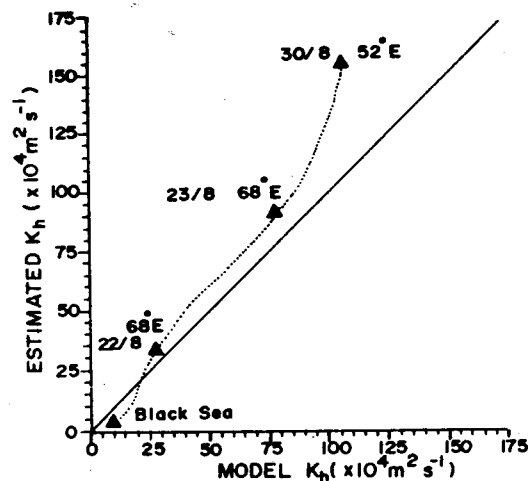


Fig. 7—Comparison of K_h computed from Methods 1 and 2 [The value of K_h computed (through Method 1) and estimated (after, Pivovarov & Protasov⁷) for the Black Sea is also included]

to strong winds in WEAS and lower turbulent mixing regime in CEAS, respectively. The large columns of homogeneous water in the upper 50 m in WEAS (Fig. 2) with strong lateral gradients in temperature also indicates that the turbulent mixing is strong along the vertical by which the transfer of heat flux reaches to greater depths. Thus one would see temperature difference of nearly 1°C in the upper 50 m water column from 0000 to 24000 hrs IST along 52°E (Fig. 2b) which indicates a considerable loss of heat in the upper 50 m [heat content decreases from 0000 to 2400 hrs IST and ΔH is negative; Eq. (11)]. This, together with the higher net surface heat flux (Table 1) on 30 August leads to the higher values of estimated K_h [from Eq. (13)] along 52°E. However, for computing K_h from the model, the entire thermal structure along 52°E is considered to separate the diurnal cycle on 30 August. The prevailing large difference of temperature and also the presence of lower temperature at 1°N along 52°E indicating the large aperiodic trend thereby effect the amplitude of diurnal variation and hence the computed K_h over the estimated K_h along 52°E in WEAS. The computed daily and depth averaged K_h of this study must be regarded as the composite effect of unstable stratification during nighttime cooling and stable stratification during daytime warming conditions.

It is worth mentioning that the advantages of the model are (i) one requires values of diurnal temperature changes only at two levels (surface and z_0) instead of temperature profiles, and (ii) one requires only the information on solar irradi-

ance below the sea surface and does not need the other information on surface meteorological observations and surface heat fluxes.

Acknowledgement

Authors are thankful to Dr E. Desa, Director, NIO and Dr N. Bahulayan, Co-ordinator, Indo-USSR Collaboration Project, at NIO, Goa, India for their keen interest in this study. They also thank Dr M.K. Antony for providing useful suggestions. One of the authors (POZ) thanks Prof. S.S. Lappo, Director, State Oceanographic Institute, Moscow and Dr E.A. Kulikov, Co-ordinator, Indo-USSR Collaboration Project for deputing him to NIO, Goa, India to participate in the cruise on board *ORV Sagar Kanya*. The help received from Dr I. Zveriaev, co-participant from USSR and other Indian participants of the cruise is acknowledged.

References

- 1 Imawaki S, Niller P P, Gautier C H, Halpern D, Knox R A, Large W G, Luther D S, McWilliams J C, Moum J N & Paulson C A, *J Geophys Res*, 93 (1988) 14005.
- 2 Lukas R, *TOGA (Tropical Ocean-Global Atmosphere) Notes*, 2 (1991) 1.
- 3 Toole J M, *J Phys Oceanogr*, 17 (1987) 1397.
- 4 Hareeshkumar P V, Pradeepkumar T, Mathew B & Joseph M X, *Indian J Mar Sci*, 19 (1990) 36.
- 5 Rao R R, Sunderaramam K V & Santa Devi M R, in *The monsoon dynamics*, edited by J Light Hill & R P Pearce (Cambridge University Press, Cambridge) 1981, pp 375.
- 6 Bowden K F, Howe M R & Tait R I, *Deep-Sea Res*, 17 (1970) 401.
- 7 Pivovarov A A & Protasov S N, *Oceanology*, 15 (1975) 291.
- 8 Zavialov P O & Rozhdestvensky A E, *Izvestiya Academy of Sciences, USSR Atmospheric and Oceanic Physics*, 27 (1991) 76.
- 9 Sverdrup H U, Johnson M W & Fleming R H, *The oceans. Their physics, chemistry and general biology* (Prentice-Hall Inc, Englewood Cliffs, New Jersey) 1942, pp 1087.
- 10 Zavialov P O, *Soviet Meteorol & Hydrol*, 4 (1992) 47.
- 11 Voskanyan A G, Pivovarov A A & Khundzhua G G, *Oceanology*, 10 (1970) 449.
- 12 Stevenson J W, *Computations of heat and momentum fluxes at sea surface during Hawaii to Tahiti Shuttle Experiment*, Technical Report No. HIG.82-4 (Hawaii Institute of Geophysics, University of Hawaii Press, Honolulu), 1982, pp 42.
- 13 Colborn J G, *The thermal structure of the Indian Ocean*, IIOE Oceanographic Monograph No. 2 (East-West Centre Press, University of Hawaii, Honolulu) 1975, pp 173.
- 14 Seckel G R & Beaudry F H, *Trans Am Geophys Union*, 54 (1973) 1114.
- 15 Payne R E, *J Atmos Sci*, 29 (1972) 959.
- 16 Kondo J, *Boundary-Layer Meteorol*, 9 (1975) 91.
- 17 Moum J N, Caldwell D R & Paulson C A, *J Geophys Res*, (1989) C2 2005.
- 18 Hoerber H, *J Phys Oceanogr*, 2 (1972) 303.